



PAM Review

Subject 68412
www.uts.edu.au

Macro to Nano: Scaling Effects of Bi_2Te_3 Thermoelectric Generators for Applications in Space

Christopher James Wallace Smith ^{1*}, James Sewell Cahill ² and Altay Nuhoglu ³

¹ Christopher.J.Smith-2@student.uts.edu.au

² James.S.Cahill@student.uts.edu.au

³ Altay.Nuhoglu@student.uts.edu.au

* Author to whom correspondence should be addressed;
E-mail: Christopher.J.Smith-2@student.uts.edu.au

DOI: <http://dx.doi.org/10.5130/pamr.v3i0.1415>

Abstract:

For decades research and development has been committed to improving the Figure of Merit (ZT) of Bismuth Telluride (Bi_2Te_3) Thermoelectric Generators (TEG) and has reached its limit at ≈ 1 . This Meta-study aims to determine if further improvements can be made when the size of TEGs decrease. To quantify the change from macro to nano scale the change in ZT, thermal and electrical conductance, Seebeck coefficient and power factor as the size of the thermoelements decrease has been investigated as well as how Wiedemann-Franz (WF) law holds on the nanoscale. This meta-study was conducted by evaluating and comparing developments in TEGs for the past three decades.

Based on theory it was expected that increases in ZT would occur as the thermoelement dimensions are reduced due to increased scattering of electrons and phonons as well as the increased density of electronic states. Increases to ZT due to these effects was not observed in experimental data due to difficulties in nanoscale production. This meta-study observed some indicators that the theory is correct in reduced thermal conduction from increased phonon and electron scattering and that phonon scattering was greater than electron scattering. Furthermore, a weak indication that WF law is not applicable on the nanoscale due to the scattering suggesting a decoupling of electrical and thermal conduction which is not achievable in macro scale TEGs

Keywords: Thermoelectric; Generator; Figure of Merit; ZT; Scaling; Macro; Micro; Nano; Bismuth Telluride; Space; Bi_2Te_3 , Meta-study

Nomenclature

CSD Thermolement Cross Sectional Dimension (μm , nm)

ZT Dimensionless Figure of Merit

S Seebeck Coefficient (V/K)

κ Thermal Conductivity ($\text{W m}^{-1}\text{K}^{-1}$)

σ Electrical Conductivity (Ωm)⁻¹

1. Introduction

Thermoelectric generators (TEGs) and Thermoelectric Coolers (TECs) are solid state devices that produce an electrical potential difference when a difference of temperature exists. TEGs operate on the Seebeck effect (Equation. 1) to generate electricity and TECs operate on the Peltier effect to create a temperature differential. The difference in temperature causes electrical current to flow, producing useful power.

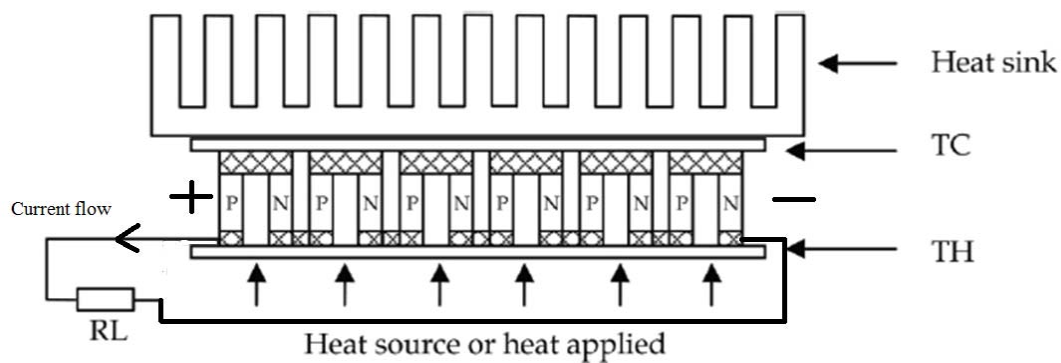


Figure 1. Diagram of a TEG showing the arrangement of the thermocouples in a typical TEG, how the Seebeck effect affects current flow, and the hot and cold sides of the TEG [1].

Due to the lack of moving parts, TEG's have been seen as attractive options for energy retrieval in waste heat recovery, such as waste heat from electronics or life support systems [2]. Furthermore TEG's have been utilised in 'thermal batteries' such as a Radioisotopic Thermoelectric Generator (RTG). RTG's use a radioactive heat source, such as Plutonium-238, and have been used in numerous deep space probes, such as the Voyager and Cassini missions, as viable collection of energy through solar panels is not feasible due to the vast distances from the probes to the sun. RTG's have also been used in terrestrial probes or rovers, such as the Curiosity Rover, as well as several experiments left on the Moon by the Apollo missions.

Unfortunately TEGs themselves are very inefficient, with efficiencies of only 3-7% usually seen. By focusing on improving the ZT (Equation. 2), we are able to improve the effectiveness of the TEG.

1.1 Seebeck Effect

The Seebeck Effect is the generation of a voltage on two dissimilar electrical conductors when the two materials are exposed to different temperatures. By electrically connecting the junctions together with an external circuit a current will flow. The current generated is proportional to the temperature gradient between the hot and cold junctions and the voltage is proportional to the temperature difference.

Heat must be dissipated from the cold junction as sufficient accumulation of heat will effectively eliminate the temperature difference across the device causing the migration, and hence the current to stop.

$$J = \sigma(-\nabla V - S\nabla T) \quad (1)$$

Equation 1 is the Seebeck equation where J is the current density, ∇V is the voltage gradient, σ is the electrical conductivity, S is the Seebeck coefficient and ∇T is the temperature gradient.

The Seebeck coefficient varies as a function of temperature and depends on the conductors' material composition. If a system reaches a steady state where $J=0$, then the voltage gradient is given by the emf: $-\nabla V = S\nabla T$. This relationship does not depend on conductivity and is used in thermocouples to measure a temperature difference; by performing the voltage measurement at a known reference temperature an absolute temperature can be found.

1.2 Figure of Merit

The Figure of Merit (ZT) is a dimensionless value used to describe the overall performance of a TEG. It is defined by:

$$ZT = \frac{\sigma S^2 T}{\kappa} \quad (2)$$

Where σ is the electrical conductivity, S is the Seebeck coefficient, T is the temperature and κ is the thermal conductivity.

Large values of ZT require high S , high σ and low κ . Since an increase in S normally implies a decrease in σ because of carrier density considerations, and since an increase in σ implies an increase in the electronic contribution as given by the Wiedemann-Franz (WF) law, (Equation 3) it is very difficult to increase Z in typical bulk thermoelectric materials.

$$\frac{\kappa}{\sigma} = LT \quad (3)$$

Equation 3 is the Wiedemann-Franz law where κ is the thermal conductivity, σ is the electrical conductivity, T is the temperature and L is the Lorenz number, a proportionality constant.

1.3 Bismuth Telluride TEG's

Bismuth telluride, Bi_2Te_3 , is a semiconductor that displays properties as a TEG. Bismuth telluride is thermally and electrically anisotropic, meaning that its thermal and electrical properties are not consistent throughout the entire material. This is due the bonds between Te and Bi atoms are strongly covalent while adjacent Te atoms are bonded by van der Waals interactions.

While the Seebeck coefficient through the material remains essentially isotropic, with a standard deviation of around 10% [3], the electrical and thermal conductivities in the vertical direction, parallel to the hot/cold junctions of the Bi_2Te_3 TEG is higher than the thermal and electrical conductivities in the horizontal direction perpendicular to the hot/cold junctions of the TEG [4]

Due to a TEGs need for low thermal conductivity, the dissipation of heat from the TEG can be severely limited. With increasing temperature, the concentration of phonons increases, which causes increased scattering. This lattice scattering lowers the carrier mobility more and more at higher temperatures [5]. As TEG's require to operate at high temperatures to be economical ($>473\text{K}$), this property is severely limiting to the operation of the TEG. Furthermore, as a high Seebeck Coefficient is required for a useable output voltage [6], an individual thermocouple does not output a enough voltage, most TEG's place a number of thermocouples in series to boost output voltage. With- each added thermocouple, the output resistance of the TEG increases. Typical TEG's have an output resistance in excess of 10 ohms [7]. Therefore only high resistance loads can generally be used for a TEG, otherwise the power is dissipated across the output resistance.

Most typical Bi_2Te_3 generators have a ZT of around 1 [3]. Many studies [8,14,15] have found that through using materials such as Antimony or Lead to dope Bi_2Te_3 can increase the ZT value. Other studies, theoretical and experimental have looked at the effects of reducing the dimensions of Bi_2Te_3 TEG's. As the TEG dimensions decreased, theoretically there should be an increase of efficiency [7].

Bi_2Te_3 is limited to a maximum hot side temperature of $\sim 820\text{K}$ [12]. Due to the deleterious effects of oxygen on these materials at high temperatures, as well as the materials high vapour pressures, the tellurides must be operated in a sealed generator with an inert cover gas, such as helium to slow the sublimation and vapour phase transport within the TEG [13].

Bulk thermal insulation is used due to the presence of the cover gas. Helium gas buildup within the converter must be controlled by using a separate container around the heat source or permeable seals in the generator design [14].

Due to the separate gas container/seals and the use of bulk insulation materials, there is an increase in the size and weight of the Bi₂Te₃ generator [13]. However, this type of TEG is particularly useful for Radioisotopic TEGs (RTG) operating in space vacuum or for planetary atmospheric applications.

1.4 Macro to Nano

Improving the ZT for TEGs requires independent optimisation of electrical and thermal conductivity (Equation 3). For bulk materials independent optimisation of thermal and electrical conductivity is impossible due to the Wiedemann-Franz Law [16]. Manufacturing a TEG on the nanoscale allows for the alteration of the mesostructure by the introduction of new thermoelement geometries that are; 2D, nano film, 1D nanowire (NW) and 0D quantum dots.

Theoretically, the ZT will be improved for nanoscale TEGs due to increased electrical conductivity and reduced thermal conductivity [17]. These effects arise from increased scattering of phonons and electrons as well as an increase in the density of electronic states near the Fermi level [18]. Compared to bulk, an array of nanowire thermoelements has an increased number of boundaries, these boundaries scatter phonons significantly more than electrons due to the larger de Broglie wavelength of electrons which is roughly an order of magnitude greater than the dominant phonons [19].

Lowering the dimensions increases the density of electronic states near the Fermi level which increases the Seebeck coefficient through a larger density of electrons at high potentials. The higher density of states increases the overall mobility of electrons which is represented by increased electrical conductivity. By restricting the movement of electrons to 1D results in a longer mean free path in the direction that does useful work, increasing efficiency for the TEG [20].

In describing thermoelectrics on the nanoscale it is important to consider the effects of decreased grain size. As the grain size within the TEG decreases, it increases the number of interfaces, or grain boundaries. The increased number of boundaries improves the ZT as detailed above, however with reduced grain size, many boundaries will have complex geometry and the amount of point defects that can exist at the boundaries increases [21]. Point defects alter the charge distribution in the lattice which greatly disrupts electron flow. Annealing makes cleaner boundaries although this process will increase the average grain size.

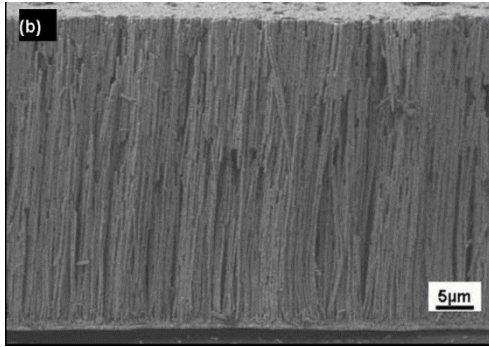


Figure 2. A typical array of nanowires. Note the wires are not uniform as some are partially complete, or have broken during manufacturing [22].

The material properties of nanowire arrays are mechanically very weak and fragile. This makes them suitable candidates for space applications as terrestrial situations would generally expose them to more stress and strain. Due to the highly reactive surface of the wires, oxidation can be an issue but not in space applications.

2. Method

Many researchers have investigated how scaling affects TEG electrical and thermal performance theoretically and by simulation. By gathering experimental data from researchers that have manufactured nano and micro sized TEGs this meta-study determines whether experimental results agree with theoretical literature.

To allow for a comparison with the bulk form it was decided to restrict the material composition of the TEGs to Bi_2Te_3 , as it has been widely researched and developed due to having the best bulk performance beaten only by its alloys. Bi_2Te_3 is also well suited to space missions as its operational temperature range applies to space, e.g. Radioisotopic TEGs.

Experimental data was gathered from research articles accessed through Science Direct (Elsevier), Access Science, ProQuest, arXiv and Google Scholar. The keywords searched were; TEG, thermoelectric, Bismuth Telluride, Bi_2Te_3 , macro, micro, nano, quantum, wire.

The initial goal was to investigate the thermodynamic parameters affecting TEG power efficiency, namely thermoelement dimensions and operational temperature. This approach was abandoned as large amounts of necessary data was consistently omitted from relevant papers.

Instead focus was shifted on the relationship between ZT and thermoelements contact surface dimension (CSD). Obtaining data on the ZT, electrical conductivity, and thermal conductivity dependence on CSD, specifically as they change from the macro to micro to nano enabling an analysis of scaling effects. These parameters were chosen as ZT is an indicator of overall efficiency and performance of TEGs, additionally limiting the amount of variables our research depended on, whilst still providing meaningful data pertaining to the improvement

of characteristics of TEGs. Graphs of ZT vs Macro-Micro-Nano CSD, Thermal Conductivity vs Nano CSD, Electrical Conductivity vs Nano CSD were plotted and Power Factor vs CSD was chosen as opposed to Seebeck Coefficient vs CSD because Power Factor fitted with our limited dataset and gave information on the power obtainable.

Due to lack of reliable data for an analysis over a range of temperatures, data sets on TEG performance at room temperature (300K) were focused on. Since Superlattices have alternating material composition and quantum dots need to be stacked to have any usefulness, we focused on nanowire arrays as it is the lowest dimensional form that can be compared to it's bulk.

3. Results

3.1 Electrical Conductivity vs CSD

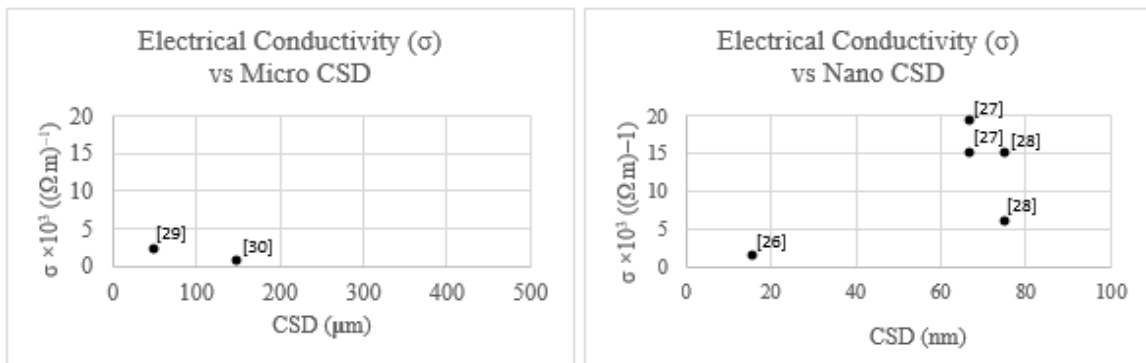


Figure 3. Electrical conductivity for micro and nano CSD. Note Micro CSD is in μm , Nano CSD is in nm.

Bulk electrical conductivity is around $50 \times 10^3 \Omega\text{m}^{-1}$ [23]. Nanowires show reduced electrical conductivity as a result of increased scattering as CSD decreases. Theoretically it will increase but difficulties in manufacturing on the nanoscale, discussed further down, causes these results. The point defects which alter the charge distribution is responsible for a significant portion of the decrease.

3.2 Thermal Conductivity vs CSD

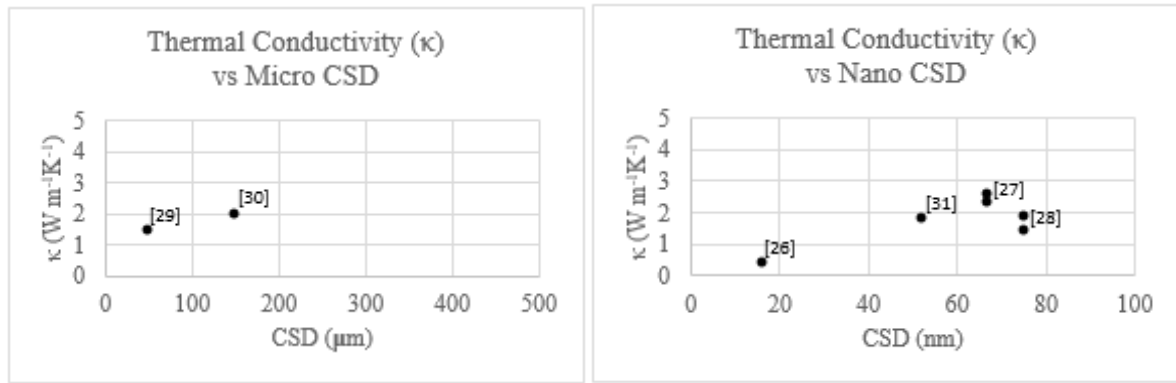


Figure 4. Thermal conductivity vs CSD for micro and nano sample.

Bulk thermal conductivity is $5.1 \text{ W m}^{-1} \text{ K}^{-1}$ [23]. Thermal conductivity shows a decrease on micro and nano scales. This is a result of the increased phonon scattering from the lower CSD of the wire which results in a shorter distance to travel before reflected phonons at the boundary interfere. Reduced electron transport which is the larger component of thermal transport also contributes to the reduction [19].

3.3 ZT vs CSD

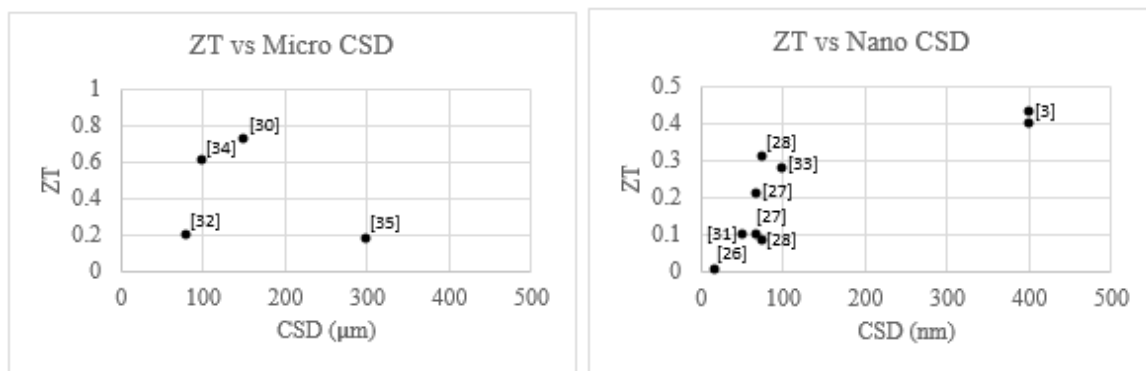


Figure 5. Graphs depicting ZT vs CSD for Micro and Nano samples.

Bulk ZT is around 1 [23]. As seen in figure 10, comparing the micro to nano graphs it is observed that as CSD decreases the ZT also decreases. This is a direct contradiction to what was expected from the theoretical literature, where it should increase. This is likely due to the significantly reduced electrical conductance from the defects in the grain structure, namely point defects which disturb the charge distribution. While thermal conductivity is reduced, the electrical is impacted more.

3.4 Power Factor vs CSD

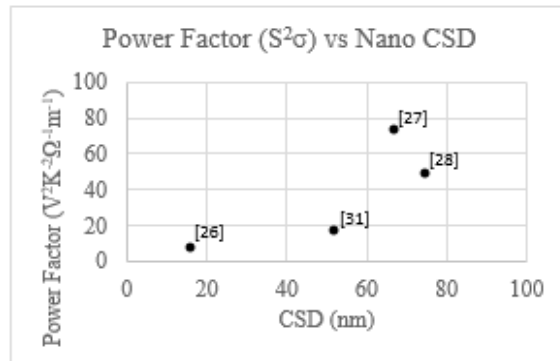


Figure 6. Power Factor vs CSD.

Bulk power factor is $1531.25 \text{ V}^2\text{K}^{-2}\Omega^{-1}\text{m}^{-1}$, over 20x higher than its nanosized counterpart. Power factor values are seen to be lower as CSD decreases and the reasons are the same for electrical and thermal conductivity.

3.5 Thermal to Electrical Conductivity Ratio vs CSD

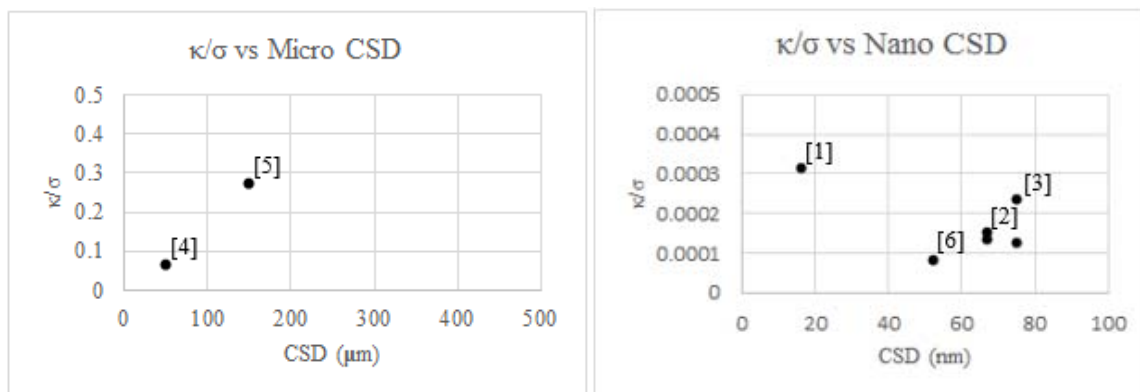


Figure 7. The ratio of thermal conductivity to electrical for micro and nano CSD.

Thermal conductivity to electrical conductivity ratio decreases as CSDs go from micro to nano. The decreasing ratio is due to a combination of the electrical conductivity being significantly reduced more than the thermal.

As bulk materials follow the Wiedemann-Franz law, their ratio of thermal conductivity to electrical conductivity is constant and equal to LT (Equation 3). The theory for nanosized TEGs is that it allows for independent alteration of thermal and electrical properties, a task prohibited by WF. It is observed that for decreasing CSDs the Lorenz number has decreased which is a violation of WF. The reasons for why electrical and thermal conductivity are

outlined in the previous graphs. This result is supportive of the theory behind nanoscale TEGs as independent alteration of electrical and thermal properties is achievable.

4. Discussion

The results obtained from experimental data shows that as the CSD decreases, ZT decreases. This discrepancy comes from the difficulties in nanoscale manufacturing which results in impurities and detrimental defects at grain boundaries.

Existence of precursor chemicals or contamination from mechanical manufacturing can cause significant degradation of the TEG [24] as introduction of contaminants either from precursors leftover after deposition, or contaminants from mechanical manufacturing process. Wet chemical deposition appears to be one of the more difficult methods of production of TEGs as it is inherently hard to remove impurities.

Mechanical methods such as ball milling offers some advantages over wet chemical, as ductile coatings on the milling equipment; or altering manufacturing speeds helps restrict the number of defects when compared to wet chemical. Vapor deposition is a direct method for preparing NW as there are no precursors but the high energy atoms can damage the sample as they make contact. Due to different thermal expansion for Bi and Te some NWs can fracture during the process.

Producing suitable electrical contacts by vapor deposition for NW array can cause damage to the wire and result in disconnections between the contacts. Electrical contacts for NWs can be achieved by a wet approach but often a large amount of impurities will exist between the wires.

Due to the high surface area of nanoparticles they are much more reactive compared to the bulk material. Therefore oxidation of the TEG material during the manufacturing process is extremely likely to occur. To mitigate excessive oxidation, the TEG must be manufactured and kept in an inert gas environment.

There is difficulty in creating clean grain boundaries for small grain size due to random crystal growth orientation. Solidifying the grains in the presence of a magnetic field aligns [3] the grains and slower temperature changes during the phase change allows for small grains that are orientated and low amounts of charge distribution affecting point defects at the boundary.

Comparing the results from macro, to micro and to nano, there is a notable reduction in thermal conductivity. Thermal conductivity is greatly influenced by the reduced dimensions as there the reflection of phonons at the wire edge increases the scatter. Thermal conductivity is also influenced by reduced electrical conductivity.

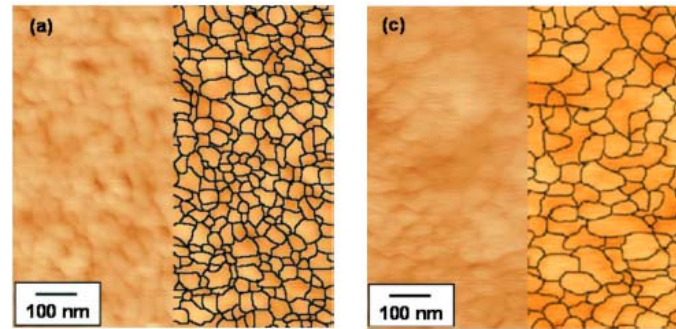


Figure 8. Surface topology and grain size of a Bi_2Te_3 sample. The image on the left shows the Bi_2Te_3 sample as manufactured (pre-annealing). The image on the right shows the same sample after being annealed at 523K for 30 mins [25].

In figure 8 the dramatic effects of annealing to the grain structure and surface topology can be seen, the annealed sample showing a smoother surface, larger grains with neat, clean interfaces when compared to pre-annealing. This figure shows annealing decreasing the amount of boundaries, reducing their complexity and the amount of defects at the interfaces. Decreases in thermal conductivity is a result of the increased amount of boundaries which allows for greater phonon scattering. While there is increased phonon scattering, the non-uniform and erratic grain boundaries also increases electron scattering due to the increased amount of point defects along the interfaces.

When the grain of the pre-annealed is compared to the annealed sample, the grain boundaries are much neater, with a greater amount of uniformity. This allows for a greater electrical conductance, but also increases the thermal conductance due to the reduced boundaries.

In the search for experimental evidence that aligns with theoretical performance as a meta study it may be more sensible to look at nanowires of a material that has a more mature nano manufacturing process such as SiGe. An alternative method for reliable production of Nano sized TEGs may be more readily available using another material. Silicon Germanium (SiGe) has been shown to be reliably manufactured, but at the cost of an inferior performing TEG, albeit experimental and theoretical evidence has shown that SiGe nanowires TEG efficiency can be improved, by changing the doping and nanowire size. This is because manufacturing methods for this technology is far more developed and matured, and so its production is far more reliable [19] This meta-study has also highlighted a need for researchers to include more data in their papers or for data not entirely relevant to the paper be easily accessible for peer review and further analysis.

4. Conclusion

Theoretical evidence suggests an improvement of ZT as the TEG CSD are reduced. The experimental evidence sourced could not support this hypothesis. This is most likely to be due to difficulties in nanoscale manufacturing and not an error in theory. The data obtained did show strong evidence of increased scattering of electrons and phonons which is the mechanic that the theory is dependent on. Weak evidence for a violation of the WF law was observed which is due to the increased scattering but importantly that electrical and thermal

conductivity are no longer entwined on the nanoscale. If there was more data available it would have enabled a more thorough meta-study but would not have changed the conclusion that nanoscale TEGs are currently unable to outperform their bulk counterparts, although theoretical modelling suggests they can if manufacturing improves sufficiently.

5. Acknowledgments

The Authors would like thank Jurgen Schulte, UTS for giving his professional expertise, assisting the progress of our meta-study. Marcel Bick, CSIRO for stimulating discussions.

6. References

1. Anon, 2016. [online] intechopen.com. Available at: <<http://www.intechopen.com/source/html/40611/media/image3.png>> Web. 9 May 2016
2. Alam, H. and Ramakrishna, S., 2013. A review on the enhancement of figure of merit from bulk to nano-thermoelectric materials. *Nano Energy*, 2(2), pp.190-212. doi: <http://dx.doi.org/10.1016/j.nanoen.2012.10.005>
3. performance analysis and economic evaluation of combined biomass cook stove thermoelectric (BITE) generator.
4. Thermoelectric Generators For Use In Space And Human Bodies - DTU Energy". <http://www.energy.dtu.dk>. N.p., 2015. Web. 14 May 2016.)
5. 4.5 Bismuth Telluride And Its Alloys". *Iue.tuwien.ac.at*. N.p., 2016. Web. 15 May 2016.
6. Manzano, Cristina V. et al. "Anisotropic Effects On The Thermoelectric Properties Of Highly Oriented Electrodeposited Bi₂te₃ Films". *Sci. Rep.* 6 (2016): 19129. Web. 9 May 2016
7. Medlin, D.L. and G.J. Snyder. "Interfaces In Bulk Thermoelectric Materials". *Current Opinion in Colloid & Interface Science* 14.4 (2009): 226-235. Web. 26 May 2016.
8. "Thermoelectric Power Generators Or Seebeck Power Generation | Electrical4u". *Electrical4u.com*. N.p., 2016. Web. 22 May 2016.
9. Brito, F. P. et al. "Analysis Of The Effect Of Module Thickness Reduction On Thermoelectric Generator Output". *Journal of Electronic Materials* 45.3 (2015): 1711-1729. Web. doi: <http://dx.doi.org/10.1007/s11664-015-4182-x>
10. Unknown,. "Thermoelectric Power Generators Or Seebeck Power Generation | Electrical4u". *Electrical4u.com*. N.p., 2016. Web. 20 May 2016.
11. Atuchin, V.V. et al. "Structural And Vibrational Properties Of PVT Grown Bi₂te₃ Microcrystals". *Solid State Communications* 152.13 (2012): 1119-1122. Web. doi: <http://dx.doi.org/10.1016/j.ssc.2012.04.007>
12. Brostow, Witold et al. "Bismuth Telluride-Based Thermoelectric Materials: Coatings As Protection Against Thermal Cycling Effects". *Journal of Materials Research* 27.22 (2012): 2930-2936. Web. doi: <http://dx.doi.org/10.1557/jmr.2012.335>
13. Nakagawa, Yusuke and Toshio Itami. "Eutectic Anomaly Of Compound Forming Bi-Te Liquids Studied By Electrical Resistivity Measurements". *MATERIALS TRANSACTIONS* 46.8 (2005): 1794-1797. Web. doi: <http://dx.doi.org/10.2320/matertrans.46.1794>
14. Guo, Xin et al. "Double Effects Of High Pressure And Sb Doping Content On Thermoelectric Properties Of Bi₂te₃-Based Alloys". *Chemical Physics Letters* 550 (2012): 170-174. Web. 26 May 2016.

15. Ryu, Byungki et al. "Prediction Of The Band Structures Of Bi₂Te₃-Related Binary And Sb/Se-Doped Ternary Thermoelectric Materials". *Journal of the Korean Physical Society* 68.1 (2016): 115-120. Web. 23 May 2016.
16. Alam, Hilaal and Seeram Ramakrishna. "A Review On The Enhancement Of Figure Of Merit From Bulk To Nano-Thermoelectric Materials". *Nano Energy* 2.2 (2013): 190-212. Web. 26 May 2016.)
17. (Hicks, L. D. and M. S. Dresselhaus. "Thermoelectric Figure Of Merit Of A One-Dimensional Conductor". *Phys. Rev. B* 47.24 (1993): 16631-16634.) doi: <http://dx.doi.org/10.1103/PhysRevB.47.16631>
18. (Kim, Jeongmin, Wooyoung Shim, and Wooyoung Lee. "Bismuth Nanowire Thermoelectrics". *J. Mater. Chem. C* 3.46 (2015): 11999-12013.)
19. (Boukai, A., K. Xu, and J. R. Heath. "Size-Dependent Transport And Thermoelectric Properties Of Individual Polycrystalline Bismuth Nanowires". *Adv. Mater.* 18.7 (2006): 864-869.). doi: <http://dx.doi.org/10.1002/adma.200502194>
20. (Yu.V. Ivanov Chapter 18 "Phonon-Drag Thermopower of Low-Dimensional Semiconductor Structures" "Thermoelectrics Handbook" Edited by D.M Rowe (2005).
21. (Liu, Yufei, Menghan Zhou, and Jian He. "Towards Higher Thermoelectric Performance Of Bi₂Te₃ Via Defect Engineering". *Scripta Materialia* 111 (2016): 39-43.). doi: <http://dx.doi.org/10.1016/j.scriptamat.2015.06.031>
22. (Kalapi G. Biswas, Vijay Rawat, Manuel DaSilva, Timothy D. Sands "Bi₂Te₃ Nanowire array/epoxy composites for thermoelectric power generators and microcoolers" Proceedings of 2 nd Energy Nanotechnology International Conference 2007)
23. (Satterthwaite, C. B. and R. W. Ure. "Electrical And Thermal Properties Of Bi₂Te₃". *Phys. Rev.* 108.5 (1957): 1164-1170.). doi: <http://dx.doi.org/10.1103/PhysRev.108.1164>
24. (Kyung Tae Kim, Tae Soo Lim, Gook Hyun Ha "Improvement in Thermoelectric Properties of N-type Bismuth Telluride Nanopowders By hydrogen Reduction Treatment" *Rev. Adv. Mater. Sci.* 28(2011) 196-199)
25. Takashiri, M. et al. "Effect Of Grain Size On Thermoelectric Properties Of N-Type Nanocrystalline Bismuth-Telluride Based Thin Films". *J. Appl. Phys.* 104.8 (2008): 084302.
26. Wang, K., Liang, H., Yao, W. and Yu, S., 2011. Templating synthesis of uniform Bi₂Te₃ nanowires with high aspect ratio in triethylene glycol (TEG) and their thermoelectric performance. *Journal of Materials Chemistry*, 21(38), p.15057. doi: <http://dx.doi.org/10.1039/c1jm12384j>
27. Shin, H., Jeon, S., Yu, J., Kim, Y., Park, H. and Song, J., 2014. Twin-driven thermoelectric figure-of-merit enhancement of Bi₂Te₃ nanowires. *Nanoscale*, 6(11), p.6158. doi: <http://dx.doi.org/10.1039/c4nr00191e>
28. Gao, J., Sun, K., Ni, L., Chen, M., Kang, Z., Zhang, L., Xing, Y. and Zhang, J., 2012. A Thermoelectric Generation System and Its Power Electronics Stage. *Journal of Electronic Materials*, 41(6), pp.1043-1050. doi: <http://dx.doi.org/10.1007/s11664-012-2034-5>
29. Wesolowski, D., Goeke, R., Morales, A., Goods, S., Sharma, P., Saavedra, M., Reyes-Gil, K., Neel, W., Yang, N. and Ablett, C., 2012. Development of a Bi₂Te₃-based thermoelectric generator with high-aspect ratio, free-standing legs. *Journal of Materials Research*, 27(08), pp.1149-1156. doi: <http://dx.doi.org/10.1557/jmr.2012.27>

30. Mavrokefalos, A., Moore, A., Pettes, M., Shi, L., Wang, W. and Li, X., 2009. Thermoelectric and structural characterizations of individual electrodeposited bismuth telluride nanowires. *J. Appl. Phys.*, 105(10), p.104318. doi: <http://dx.doi.org/10.1063/1.3133145>
31. Jeyashree, Y., Saptarshi, M. and A. Vimala, J., 2016. Improved Power Generation of Micro Thermoelectric Generator Using Microfluidic Heat Transfer System. *ARPN Journal of Engineering and Applied Sciences*, 10(9), pp.4302-4305.
32. Zhang, T., Chen, J., Jiang, J., Li, Y., Li, W. and Xu, G., 2011. Thermoelectric Properties of the Bi₂Te₃ Compound Prepared by an Aqueous Chemical Method Followed by Hot Pressing. *Journal of Electronic Materials*, 40(5), pp.1107-1110. doi: <http://dx.doi.org/10.1007/s11664-011-1551-y>
33. Bulman, G., Siivola, E., Shen, B. and Venkatasubramanian, R., 2006. Large external ΔT and cooling power densities in thin-film Bi₂Te₃-superlattice thermoelectric cooling devices. *Appl. Phys. Lett.*, 89(12), p.122117. doi: <http://dx.doi.org/10.1063/1.2353805>
34. Glatz, W., Schwyter, E., Durrer, L. and Hierold, C., 2009. Bi₂Te₃-Based Flexible Micro Thermoelectric Generator With Optimized Design. *Journal of Microelectromechanical Systems*, 18(3), pp.763-772. doi: <http://dx.doi.org/10.1109/JMEMS.2009.2021104>
35. Salemi, M., Toprak, M., Li, S., Johnsson, M. and Muhammed, M., 2012. Synthesis, processing, and thermoelectric properties of bulk nanostructured bismuth telluride (Bi₂Te₃). *J. Mater. Chem.*, 22(2), pp.725-730. doi: <http://dx.doi.org/10.1039/C1JM13880D>
36. Kim, D., Kim, C., Ha, D. and Kim, H., 2011. Fabrication and thermoelectric properties of crystal-aligned nano-structured Bi₂Te₃. *Journal of Alloys and Compounds*, 509(17), pp.5211-5215. doi: <http://dx.doi.org/10.1016/j.jallcom.2011.02.059>



©2016 by the authors. This article is distributed under the terms and conditions of the Creative Commons Attribution 4.0 International License (<http://creativecommons.org/licenses/by/4.0/>).